International Journal of Biological Macromolecules 264 (2024) 130453

Contents lists available at ScienceDirect

International Journal of Biological Macromolecules

journal homepage: www.elsevier.com/locate/ijbiomac

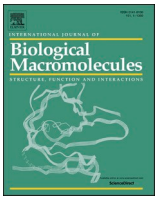

Aldehyde group pendant-grafted pectin-based injectable hydrogel

De-qiang Li *, Maryamgul Tohti, Yong-sheng Fu, Yue Zhang, Zi-wei Xiong, Jun Li *, Yan-Feng Guo

College of Chemistry and Chemical Engineering, Xinjiang Agricultural University, Urumchi 830052, Xinjiang, PR China

ARTICLE INFO

Keywords:
Pectin
Chemical modification
Imine bonds
Injectability
Self-healing
Drug delivery

ABSTRACT

Periodate oxidation has been the widely accepted route for obtaining aldehyde group-functionalized polysaccharides but significantly influenced the various physicochemical properties due to the ring opening of the backbone of polysaccharides. The present study, for the first time, presents a novel method for the preparation of aldehyde group-functionalized polysaccharides that could retain the ring structure and the consequent rigidity of the backbone. Pectin was collected as the representative of polysaccharides and modified with cyclopropyl formaldehyde to obtain pectin aldehyde (AP), which was further crosslinked by DL-lysine (LYS) via the Schiff base reaction to prepare injectable hydrogel. The feasibility of the functionalization was proved by FT-IR and ^{1}H NMR techniques. The obtained hydrogel showed acceptable mechanical properties, self-healing ability, syringeability, and sustained-release performance. Also, as-prepared injectable hydrogel presented great biocompatibility with a cell proliferation rate of 96 %, and the drug-loaded hydrogel exhibited clear inhibition of cancer cell proliferation. Overall, the present study showed a new method for the preparation of aldehyde group-functionalized polysaccharides, and the drug-loaded hydrogel has potential in drug release applications.

1. Introduction

Tumor is a malignant disease threatening human health. Currently, the main treatment methods for tumors include surgical resection, chemotherapy, and radiotherapy [1]. Among them, chemotherapy is a conventional treatment method that plays an essential and irreplaceable role in tumor treatment [2,3]. During chemotherapy, the cancer cells and normal cells are simultaneously damaged, resulting in apparent side effects [3]. Many candidate compounds or drugs currently developed or used for clinical tumor therapy have many problems, which cannot fully meet the clinical needs of tumor therapy, including strong hydrophobicity, low bioavailability, instability, large toxicity and side effects, lack of targeting, etc. [4–7]. Therefore, the approaches that can overcome the abovementioned disadvantages need to be developed and have attracted a surge of interest. Drug delivery systems can effectively reduce the release rate of drugs in the human body and prolong the release time, thus significantly improving the efficacy and safety of drugs.

Hydrogel, a three-dimensional polymer network, is considered a "solid" material with micro-scale fluidity and, therefore, has been developed as an effective carrier for delivering drugs, which showed excellent potential in drug delivery applications, as well as the studies of diagnosis, chemotherapy, and tissue engineering [8,9]. Conventional hydrogels are generally used as oral drug delivery carriers which improved the disadvantages such as bioavailability, sustained-release performance, and biocompatibility as the result of the strong chemical crosslinking that endows hydrogel with acceptable mechanical strength. However, the swelling behaviour of hydrogel in the digestive tract induces inevitable damage to the loaded drugs [10].

Injectable hydrogels are an important branch of hydrogel. Compared with conventional hydrogels, subcutaneous implantation of drug-loaded injectable hydrogels can facilely achieve the purposes, including local and site-specific effects, long administration time, and small dosage [11,12]. It has become the research hotspot of drug delivery applications for tumor treatment [13]. Many polysaccharides have been used to prepare injectable hydrogels-based drug delivery systems due to their cytocompatibility, degradability, low toxicity and stability, such as cellulose, sodium alginate, chitosan, and pectin [14–19]. Fluidity is an important index for an injectable hydrogel to present the syringeability but is limited by the strong chemical crosslinking of the polysaccharide-based hydrogel. If the polysaccharides-based hydrogels have self-healing properties, they can still retain the various performances of hydrogel after the destruction in the process of injection [20]. Dynamic covalent bonds have been widely employed to form hydrogels with self-healing properties, which can be obtained via the Schiff base reaction,

* Corresponding authors.
E-mail addresses: lsx20131120a@163.com (D.-q. Li), junli107@163.com (J. Li).

https://doi.org/10.1016/j.ijbiomac.2024.130453
Received 22 November 2023; Received in revised form 10 February 2024; Accepted 24 February 2024
Available online 1 March 2024

Diels-Alder reaction, etc. [21–24]. Thereinto, the Schiff base reaction seems to be the most appropriate route, because almost all the polysaccharides have vicinal diols that can be selectively oxidized to dialdehydes by periodate oxidation. Moreover, other part of feedstocks has the advantage of a wide range of sources, such as protein, amino acids, chitosan, polyvinylimide, and hydrazines [25–28]. However, the ring-opening reaction significantly reduces the rigidity of the backbone of polysaccharides, going against the mechanical strength of the hydrogels [29].

A facile route that can prepare the aldehyde-functionalized polysaccharides without broking the vicinal diols may retain the consequent rigidity of the backbone, resulting in a higher mechanical strength than the hydrogels from periodate oxidized polysaccharides. Thus, we prepared aldehyde group pendant-grafted pectin (AP) via etherification under alkaline conditions. In the present study, pectin was collected as the representative due to positive physiological effects, and cyclopropyl formaldehyde was used as the etherifying agent. The feasibility of etherification was proved by the FT-IR and ^{1}H NMR techniques. The AP was further crosslinked by DL-lysine (LYS) to prepare hydrogels via Schiff base reaction. The microstructure, gelation behaviour, mechanical strength, self-healing performance, and cytocompatibility were calculated. Also, the 5-fluorouracil (5-FU) was loaded on the hydrogel, and the sustained-release performance and the inhibitors of cancer cell growth were also determined. The present study showed the significance of the novel preparation route of aldehyde-functionalized pectin, and the injectable hydrogel presented excellent potential in drug delivery applications. What's more, this route for aldehyde functionalization can be popularized to all other polysaccharides to obtaine polysaccharide-based hydrogels, films, matrix, etc.

2. Materials and methods

2.1. Materials

Pectin with an average molecular weight of 37.2 kDa and a degree of esterification of 27.3 % was purchased from Macklin Biochemical Technology Co., Ltd. (Shanghai, China). NaOH was acquired from Zhiyuan Chemical Reagent Co., Ltd. (Tianjin, China). Cyclopropyl formaldehyde was obtained from Aladdin Biochemical Technology Co., Ltd. (Shanghai, China). DL-lysine was acquired from Heowns Biochemical Technology Co., Ltd. (Tianjin, China).

2.2. Preparation of aldehyde group pendant-grafted pectin (AP)

The reaction scheme of AP is shown in Fig. 1A. Five grams of pectin was dispersed in 300 mL of NaOH solution (10 wt%) with stirring for 1 h at 300 rpm to make pectin evenly dissolve. Then, 5 mL of cyclopropyl formaldehyde was dropwise added into the pectin solution in 2 min, and the reflux reaction was maintained at 50 °C for 6 h, followed by adjusting the pH of the reaction system to 6–8 with acetic acid. Finally, centrifugation (10,000 rpm), washing (ethanol solution, 90 wt%, 3 times), and freeze-drying (−40 °C) were continuously performed to obtain the AP.

2.3. Preparation of AP-LYS injectable hybrid hydrogels

Hydrogels were prepared by Schiff base reaction using AP as raw material and LYS as crosslinker. The reaction and preparation diagram of the hydrogel are shown in Fig. 1B and Fig. 1C, respectively. AP and LYS were dissolved in deionized water to obtain the AP and LYS solutions with concentrations of 10 wt% and 20 wt%, respectively. The as-prepared solutions were mixed according to the mass ratio of AP to LYS of 1: 1, 1: 2, and 2: 1. Then, the pH of mixed systems were adjusted to 8, stirred at 300 rpm for 2 h, and aged at 60 °C for another 3 h. Finally, the as-prepared hydrogels were stood at room temperature for 5 h. The obtained hydrogels were named AP1-LYS1, AP1-LYS2, and AP2-LYS1 according to the different ratios of AP to LYS.

2.4. Characterization

Pectin, AP, and the obtained hydrogels were characterized by Fourier transform infrared (FT-IR) spectroscopy. Pectin and AP were

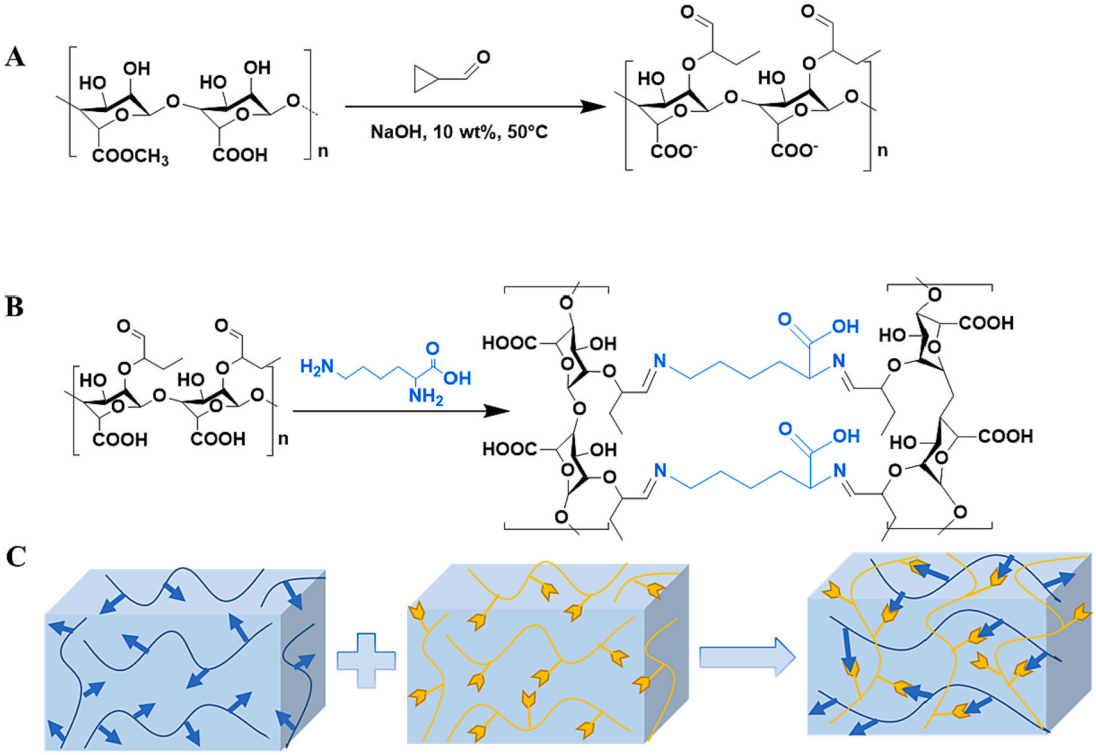

Fig. 1. The scheme of the reaction: (A) Scheme of AP preparation; (B) Scheme of hydrogel preparation; (C) Diagram of preparation of hydrogel.

also characterized by the proton nuclear magnetic resonance (^{1}H NMR) technique) performed on an AVANCE III 600 NMR spectrometer (Bruker, Germany). The micromorphology of the as-prepared hydrogels were screened by a scanning electron microscope (SEM, Hitachi S-4800, Japan). Also, we determined the gelation times of the AP-LYS injectable hybrid hydrogels by the tube-inversion method at room temperature. Mechanical properties and self-healing performances of the AP-LYS hydrogels were determined by rheological analysis on a rheometer (MCR302, Anton Paar, Austria) with a parallel plate geometry. In addition, the self-healing performances were also obtained via the macroscopic self-healing tests. pH-responsiveness property of hydrogels were calculated on an UV–Vis spectroscopy. The in vitro sustained release performace of the 5-FU-loaded hydrogel were calculated in the PBS solutions with pH of 6.8 and 7.4. The cytocompatibility of hydrogel was determined by the MTT assay, during which the L929 cell was employed and the fluorogram was obtained by IX71 fluorescence microscopy (Olympus Corporation, Japan). Also, the MCF-7 cell lines were used to calculate the inhibitory effect on cancer cells by the MTT assay test. The detailed operations are shown in the Supporting Information.

3. Results and discussions

3.1. Characterization

Fig. 2A shows the FT-IR spectrums of pectin, AP, and the resultant hydrogel. It can be seen from the pectin spectrum that the characteristic peaks of the stretching vibrations of O—H and C-OH were located at 3400 cm^{-1} and 1076 cm^{-1}, respectively. Moreover, the stretching vibrations of C═O in the methyl ester and carboxylate can be found at 1745 cm^{-1} and 1631 cm^{-1}. In the AP spectrum, the peak at 1745 cm^{-1} disappeared, indicating the hydrolyzation of the ester group under alkaline conditions. More importantly, two peaks were generated in the range of 2830–2720 cm^{-1}, which were ascribed to the stretching vibration peak of aldehyde groups. We can also find that the peak at 1631 cm^{-1} shifted to 1600 cm^{-1}, which may be induced by the aldehyde-enol tautomerism [26]. In comparison, the characteristic peaks of aldehyde have disappeared, and the peak pattern of hydroxyl groups has been unsymmetrical, indicating the generation of imine via Schiff base reaction.

This modification of pectin via the etherification reaction was first reported, and thus, we performed the ^{1}H NMR characterization to further prove the feasibility of this route. Fig. 2B shows the spectra of pectin and AP. The signals at 5.08 ppm, 4.65 ppm, 4.21 ppm, 4.06 ppm, and 3.82 ppm were responsible for the H1, H5, H4, H3, and H2 protons, respectively [30]. Moreover, some signals did not ascribe to the galacturonic acid can be found at 5.41 ppm, 2.11 ppm, and 1.19 ppm were the signals of H1 of rhamnose, acetyl groups that are binding at 3-O galacturonic acid, and methyl groups of L-rhamnose [31,32]. In the characterization of AP, the MA that possessed two olefin protons was used as the internal standard, which signal can be found at 6.29 ppm. The generated signal at 2.23 ppm is the methylene proton originating from the ring-open reaction of cyclopropyl. Also, we calculated the content of the aldehyde group from Eq. 1 and obtained a result of 0.758 mmol/g.

3.2. Micromorphology of the as-prepared hydrogels

The chemical crosslinked hydrogels can form pore structures that were the storage location for the drug models [33]. Thus, we performed SEM characterization of lyophilized hydrogels to observe their morphology (Fig. 3). It is clear that all the lyophilized hydrogels presented a three-dimensional network structure with inhomogeneous pores that were expressed in the aperture diameter. This phenomenon may be due to the rapid and nonselective electrostatic attractions between the carboxyl groups and amidogen that induced the uneven distribution of LYS on AP. However, the three-dimensional network structure endowed the as-prepared hydrogels with encapsulation capability to drugs, as well as sustained release. Compared with the other two samples, AP2-LYS1 had a more pore pile structure and the aperture were smaller that contribute to the adsorption toward drug molecules. As a result, the AP2-LYS1 may show the best sustained release performance.

3.3. Determination of gelation time

Gelation time is an essential aspect of the availability of hydrogels as biomaterials. The macroscopical gelation is shown in Fig. 4A, and the gelation times are shown in Fig. 4B. It can be seen that the gelation time increases with the decrease in AP content, indicating that the more

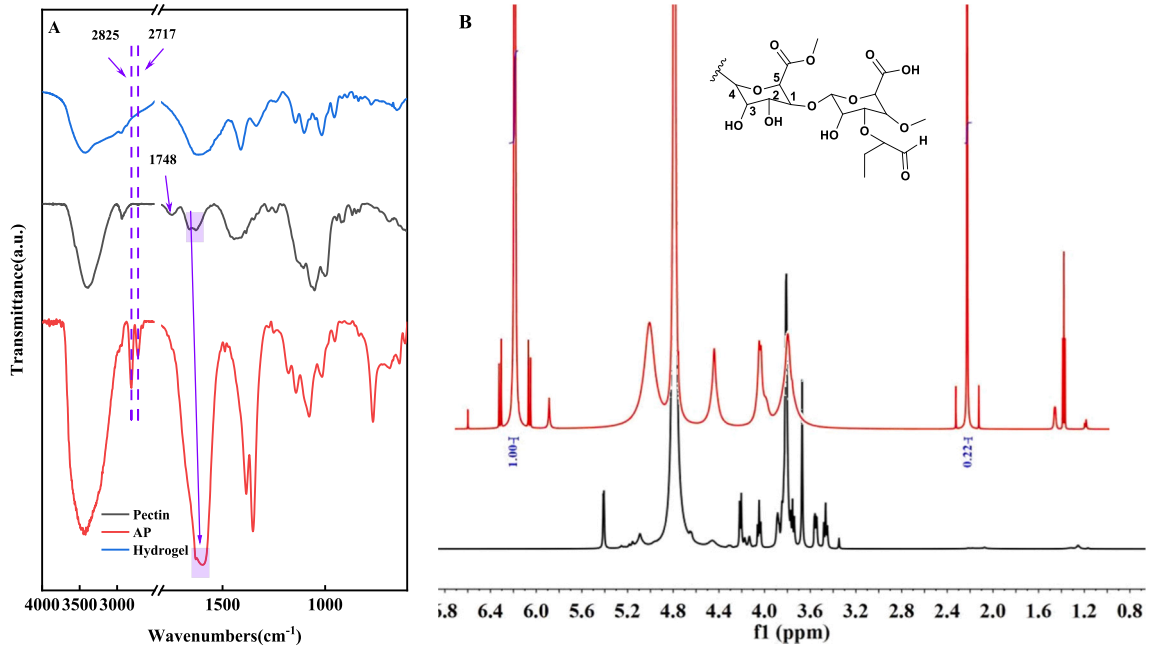

Fig. 2. Chemical characterization: (A) FT-IR spectra of the pectin, AP, and the resultant hydrogel; (B) quantitative ^{1}H NMR spectroscopy for pectin and AP.

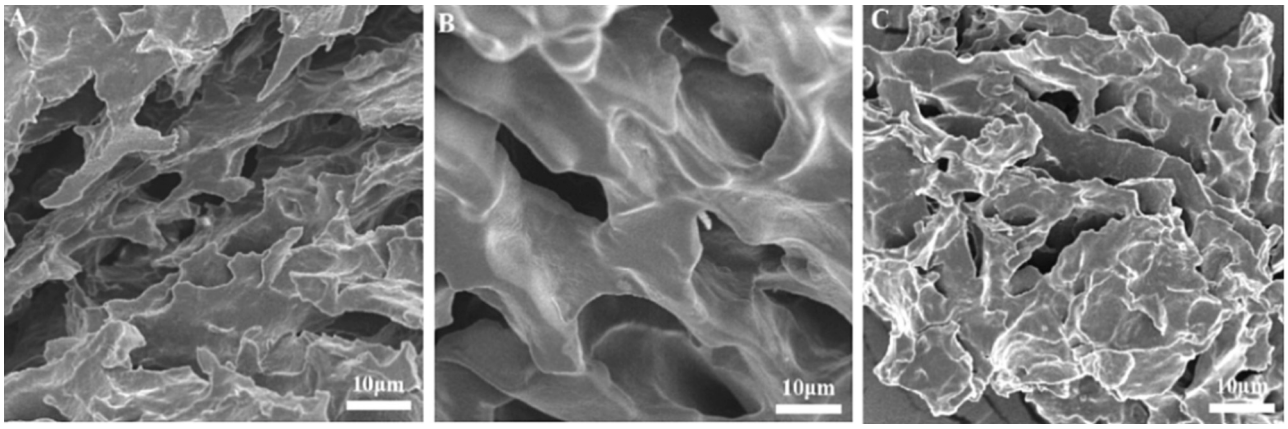

Fig. 3. SEM images (×1000) of the lyophilized hydrogels at different proportions: (A) AP1-LYS1; (B) AP1-LYS2; (C) AP2-LYS1.

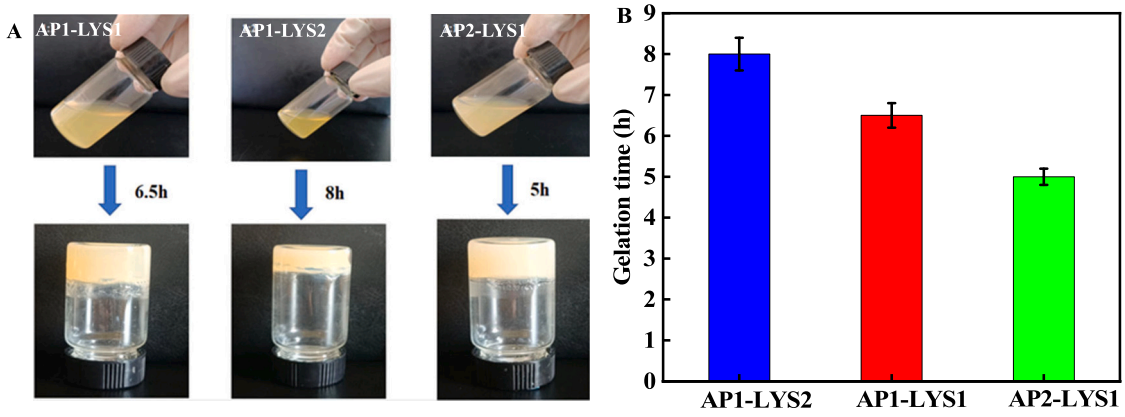

Fig. 4. Gelation process of the as-prepared hydrogels: (A) images of the gelation process; (B) Gelation time of hydrogels at different proportions.

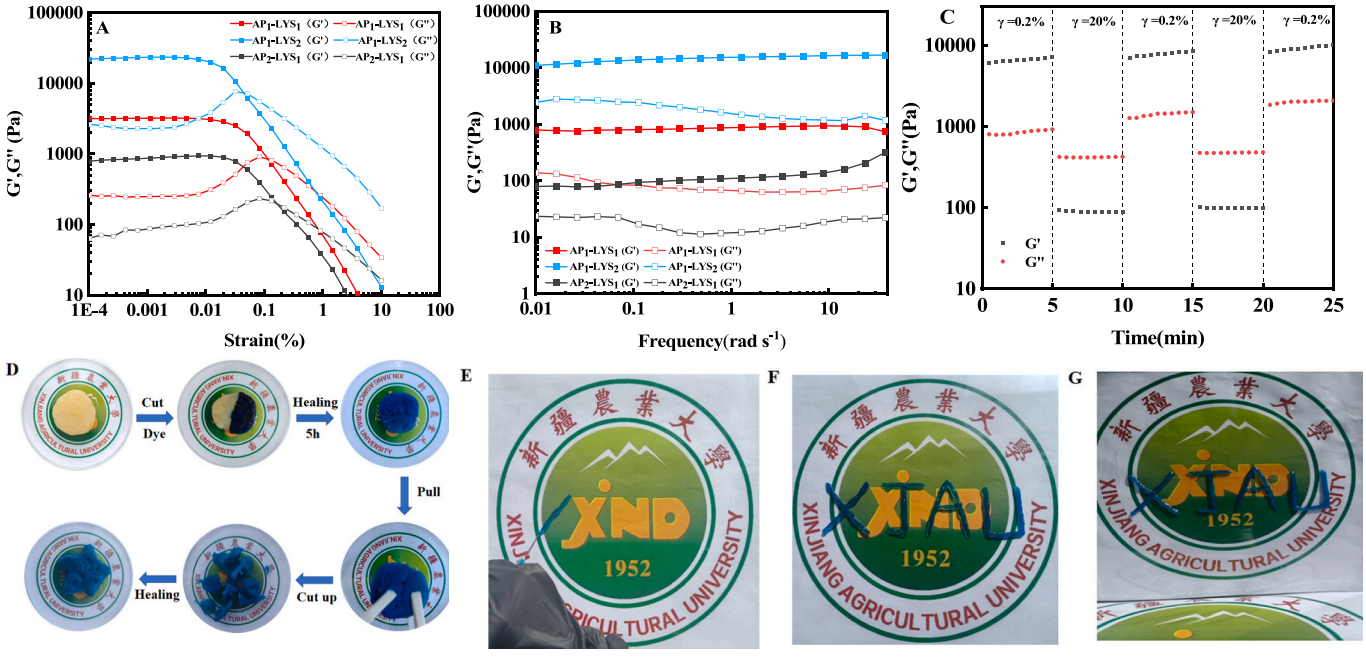

Fig. 5. Rheology and self-healing properties of the injectable hydrogels: (A) strain sweep test; (B) frequency sweep test; (C) continuous step-strain measurements of the hydrogel; (D) schematic diagram of the self-healing mechanism; (*E*-G) the macroscopical injectability test of AP1-LYS2.

content of the aldehyde group contributed to the gelation. In other words, the high content of aldehyde groups is conducive to the effective collision of chemical reactions, viz. the Schiff base reaction. Also, we recorded videos about the gelation of oxidized pectin-LYS. It is clear the oxidized pectin cannot be crosslinked by LYS and the mixture always maintain the fluidity of the liquid (Supporting Information, S2). These results indicated that the AP was more likely to form a hydrogel compared with oxidized pectin, because the AP retained the ring structure in the skeleton. Kratchanova et al. studied the chemical reactions and physical interaction of pectin in the prensence of amino acids and other amino compounds [34]. Results declared the chemical reactions (e.g., amidation, esterolysis, and degradation) and physical interactions (i.e., electrostatic interaction). Thus, we also prepared pectin-LYS composites that behaved as a fluid, indicating the inapplicability as the drug delivery carrier (Supporting Information, S3). All the results proven the significance of PA in formation of hydrogel with polyamino compounds.

3.4. Mechanical properties of hydrogels

The chemical crosslinking contributed to the forming of the pore structure of a hydrogel and also influenced the mechanical properties. Generally, a chemically crosslinked hydrogel presented high mechanical properties but delayed the degradation. Thus, the mechanical properties cannot be high for an injectable hydrogel. The present study showed the results of mechanical properties (i.e., storage modulus (G') and loss modulus (G")) obtained from the rheology of the as-prepared hydrogels under different conditions.

Fig. 5A is the results of the strain sweep test on AP1-LYS1, AP1-LYS2, and AP2-LYS1. In the low strain range, the G' was much more significant than G" of the as-prepared hydrogels, and the modulus showed slight change, indicating that hydrogels have elastic behavior and solid-like properties at this time. With the increase in the strain, the G' curves and G" curves intersected, which indicated the collapse of the hydrogel network and a gel-sol transition [35]. Moreover, the initial G' was much higher than that of the pectin-based physical hydrogels [15,16,36–38], indicating the positive role of chemical crosslinking in mechanical strength.

Fig. 5B shows the G' and G" of the hydrogel as a function of frequency (ω) at 0.2% strain. All the as-prepared hydrogels also behave as $G' > G"$, showing the dominant role of elastic module rather than viscous module in these injectable systems. Compared with the full pectin-based injectable hydrogel [27], the G' and G" of present hydrogels all showed stability to the frequency, which indicated the well crosslinking. Moreover, the three injectable hydrogels expressed significant differences in the G', viz., the G' of AP1-LYS2 was high above 10,000 Pa, and the G' of AP2-LYS1 was only 100 Pa, which manifested the LYS dosage contributed to the higher G' of the hydrogels.

3.5. The self-healing performance of the hydrogel

The self-healing performance of hydrogel was also studied, as shown in Fig. 5C. The G' was lower than G" at high strain (20%) and G' was higher than G" at low strain (0.2 %). Additionally, the G' could rapidly recover to the original value when the oscillating pressure switched from 20 % to 0.2 %. This result indicated the well self-healing properties of AP1-LYS2. The self-healing performance of the AP1-LYS2 was also determined via the macroscopic test, and the results are shown in Fig. 5D. It is clear that the two parts of the hydrogels have well self-healed and can be pulled by tweezers without fissuration. Also, we could find that the unstained part changed to blue via diffusion based on the concentration gradient of methylene blue. The chopped hydrogels likewise stuck together. All these results manifested the great self-healing performance of the hydrogel.

The injection process can be divided into two steps, viz. the failure and self-healing stages. If a hydrogel had great syringeability, it would still remain round appearance when it was extruded from the injector. It is clear the hydrogel could be facilely injected from the needle (0.45 mm) and expressed a round appearance without breakage. Moreover, the "XJAU" can be written smoothly on the glass plate, which did not show fluidity when the glass was put up. When the hydrogel was injected from the needle, the dynamic imine linkage may be broken, followed by resynthesis from the generated amine and aldehyde groups [39].

3.6. pH-responsiveness of hydrogels

As a drug delivery carrier, the stimulus-responsivenesses of the as-prepared hydrogel are expectant, such as the thermo- and pH-stimulus responsiveness. The UV–Vis spectra can be used to detecte the change of electron cloud density under different conditions, and the wavelengths of maximum absorbance were generally used as a criteria. Here, we calculated the pH-stimulus responsiveness by measuring the wavelengths of maximum absorbance, and the results are shown in Fig. 6.

The dynamic imine linkages showed differences in stability at media with different pH. Pectin, an anionic polysaccharide, also possessed abundant carboxyl groups and consequently present pH-responsiveness. The changes in of maximum absorbance wavelengths are shown in Fig. 6A. It is clear the wavelength significantly shifted with adjusting the pH of the media, indicating the pH-responsiveness of the as-prepared hydrogels. Imines generally stabilize in the near-neutral and diluent basic media and hydrolyzed under acidic conditions [40]. In detail, the hydrolyzation of imines rapidly occurred when the pH of the media was below 7, showed step-down trends in the pH range of 7–9, and then achieved equilibrium till the pH of the media reached 12 [41]. As shown in Fig. 6A, we can find four stages with the change in pH (i.e., >10, 8–10, 6–8, < 6) that differed from the abovementioned results in the neutral and diluent acidic regions. These differences may be induced by the existence of carboxyl groups that can be considered amphoteric compounds from the Lewis acid-base theory. Moreover, the reversible reaction mechanism of pectin imine in the acidic media is shown in Fig. 6B, which shows the importance of proton.

3.7. Drug release performance in vitro

5-FU is one of the most important chemotherapeutic drugs but has many side effects. Thus, we proposed to load 5-FU on the injectable hydrogels to decrease its dosage. The sustained release performances were also determined in the simulated media with different pH (i.e., 6.8 and 7.4) (Fig. 7). All the sustained release systems have cumulative release ratios below 10 % in the first 10 min, indicating that they do not occur the burst effect in the initial stage of the drug release. Moreover, the cumulative release ratio in the medium with pH = 7.4 was lower than that in the medium with pH = 6.8, which corresponds to the study of pH-responsiveness. The AP1-LYS2 obtained its release equilibrium in 8 h, and all the equilibrium release ratios were around 30 %, an excellent value for a drug delivery system. Compared with other drug delivery systems obtained from the periodate-oxidized pectin [28,30], the presently prepared drug delivery systems showed much better results in either brust release or release equilibrium. These results may reflect the advantage of the pendant grafting over the ring-opening reaction.

3.8. The cytocompatibility of the injectable hydrogels

Excellent cellular compatibility is an essential condition for the application of materials in biomedicine and drug delivery. Thus, the cytocompatibility of AP1-LYS1, AP1-LYS2, and AP2-LYS1 was calculated via the MTT method. Figs. 8(A-C) indicated that the cell proliferation rates decreased with the increasing dosage of as-prepared hydrogels. Also, the high dosage of pectin aldehyde went against cell proliferation, indicating the adverse effect of aldehyde groups. However, the lowest cell proliferation rate in the present study was still up to

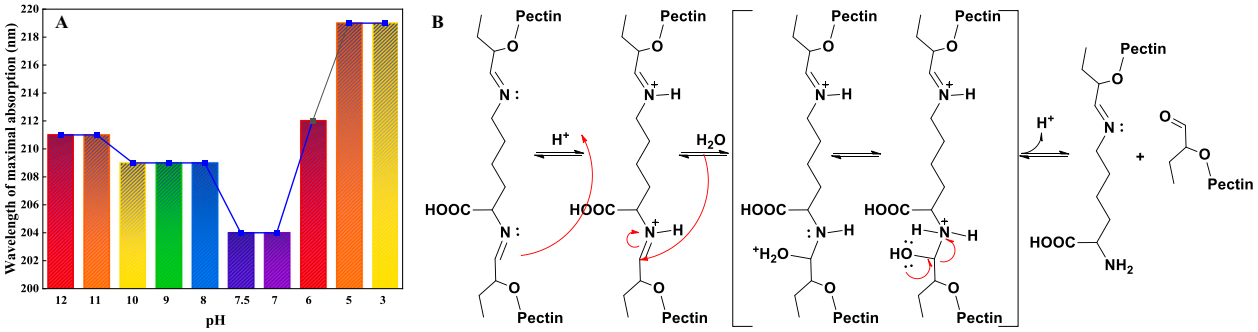

Fig. 6. The wavelength of maximal absorption of the AP1-LYS2 under different conditions: (A) media with different pH; (B) the reversible reaction of pectin imine in the acidic media, i.e., the dynamic covalent bonding.

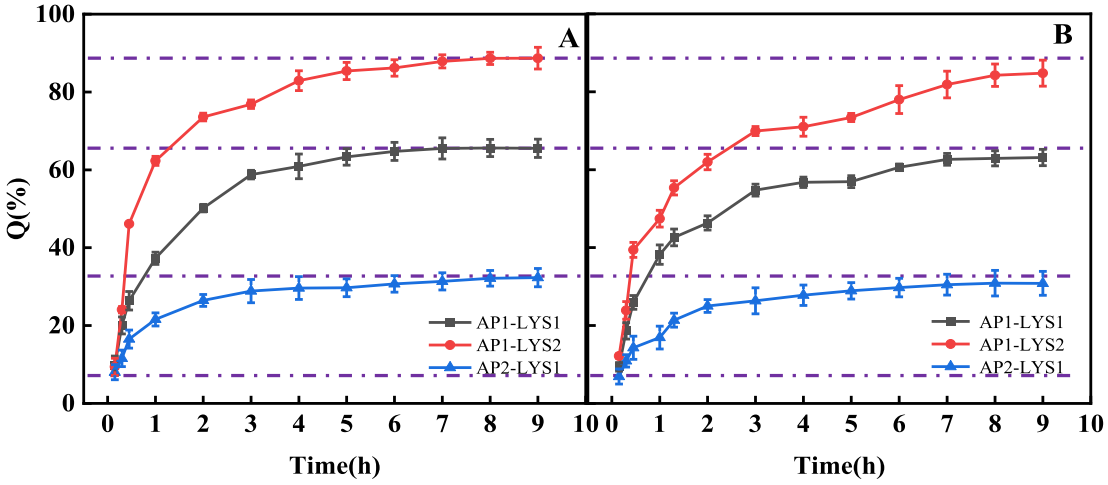

Fig. 7. Cumulative release ratio of 5-FU in different simulated media: (A) pH = 6.8; (B) pH = 7.4.

83 % after 24 h culture. When the culture time was extended to 72 h, the proliferation rate decreased to 78.32 % ± 2.14 %. When the concentration was preset as 0.225 mg/mL, the CPR value are all higher than 96 % after a 24 h of culture. Khan et al. prepared poly(N-Isopropylacrylamide)/carboxymethyl chitosan composite drug delivery carriers and studied their cytocompatibility [42]. Results showed that our carriers (0.225 mg/mL) showed much better cytocompatibility than their carrier (1 μg/mL) with a higher cell viability (96 % vs. 90 %). Anitha et al. prepared carboxymethyl chitosan nanoparticles that showed similar result cmpared with the present study [43]. These results indicated that the present injectable hydrogels had high cytocompatibility and biocompatibility to some extent. Figs. 8(D—F) show the photofluorogram of the cultured cell, from which we can find that the green spot was uniformly dispersed and the red spots were barely seen. These results also verified the high cytocompatibility of the as-prepared hydrogels.

3.9. Inhibitory effect on MCF-7 cells

From the inhibition assay on cancer cells shown in Fig. 8(G-I), it was found that the drug-loaded gel had an inhibitory effect on cancer cells, and the inhibitory effect on cancer cells was better when the gel concentration was significant because of more dosage of 5-FU. Moreover, the cell proliferation rates also decreased with the extension of culture time. After 72 h culture, the highest inhibitory rate was about 24 %. Khan et al. studied inhibition ratio of free 5-FU with a concentration of 5 μg/mL toward MCF-7 cell and found that the cell proliferation rate was close to 90 % [42]. This results showed that the present drug delivery systems can not only achieve the inhibition but sustained the release of 5-FU. Moreover, the dosage of 5-FU in the present study (4.5 μg/mL) was much lower than the clinical medication (~15 mg/kg day) and published data [44]. Thus, we can declare that this drug delivery can achieve the purpose of anticancer.

4. Conclusion

The present study developed a novel route for forming pectin aldehyde that was further cross-linked by LSY to form the injectable hydrogel. The present study has obtained several conclusions as follows.

(1) the pectin could be facilely modified with cyclopropyl formaldehyde to form the aldehyde group pendant-grafted pectin, which avoided the ring-opening reaction by periodates and can be promoted to the modification of all other polysaccharides;
(2) the AP was crosslinked by LSY via the Schiff base reaction to form the hydrogels that presented G' of >10,000 Pa with excellent self-healing performances, as well as pH-responsiveness, indicating the successful synthesis of the injectable hydrogel.
(3) the 5-FU was in situ loaded on the injectable hydrogels that have shown advantages in the burst release (< 10 %) and sustained release with only 30 % release ratios in 10 h.

CRediT authorship contribution statement

De-qiang Li: Writing – review & editing, Writing – original draft, Resources, Methodology, Investigation, Funding acquisition, Data curation, Conceptualization. **Maryamgul Tohti:** Writing – review & editing, Writing – original draft, Resources, Methodology, Investigation,

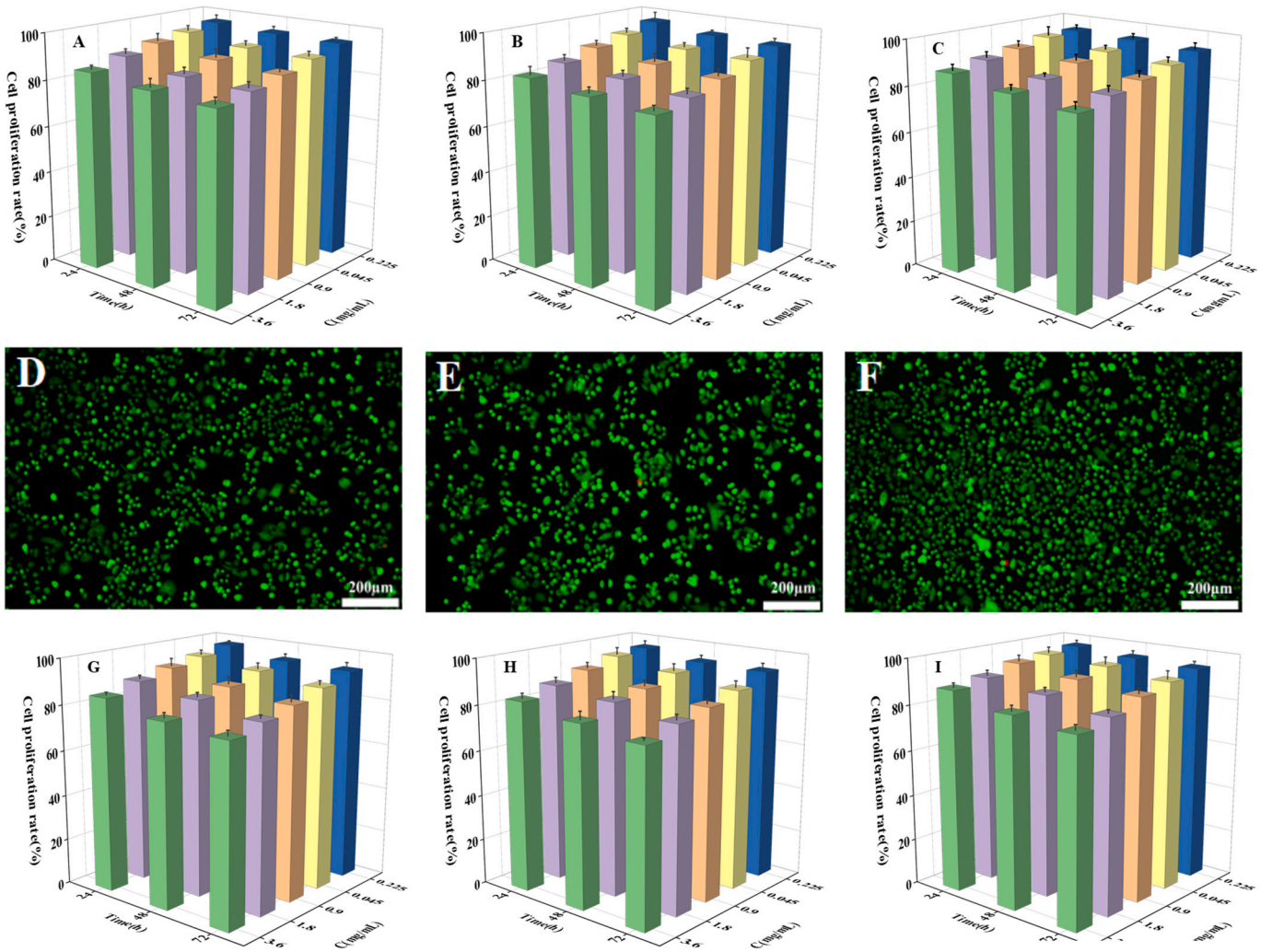

Fig. 8. MTT assay for the cytocompatibility to L929 cell and inhibitory effect to MCF-7: (A-C) the cytocompatibility of AP1-LYS1, AP1-LYS2, and AP2-LYS1, where the culture time and concentrations were the variables; (D-E) fluorogram of L929 cells in the presence of AP2-LYS1 (3.6 mg/mL) after different culture times (i.e., 24, 48, and 72 h); (G-I) MCF-7 cell proliferation rate at different culture times (i.e., 24, 48, and 72 h) in the presence of AP1-LYS1, AP1-LYS2, and AP2-LYS1 with different concentrations.

Funding acquisition, Data curation, Conceptualization. **Yong-sheng Fu:** Writing – review & editing, Methodology, Investigation, Funding acquisition, Data curation, Conceptualization. **Yue Zhang:** Writing – review & editing, Resources, Funding acquisition, Data curation, Conceptualization. **Zi-wei Xiong:** Writing – review & editing, Writing – original draft, Investigation, Funding acquisition, Data curation, Conceptualization. **Jun Li:** Writing – original draft, Methodology, Investigation, Funding acquisition, Data curation, Conceptualization. **Yan-Feng Guo:** Writing – original draft, Data curation, Conceptualization.

Declaration of competing interest

The authors declare no competing financial interests.

Data availability

Data will be made available on request.

Acknowledgment

The present work was supported by the Project of Tianshan Innovation Team Plan (No. 2023D14020) and The Youth top talent program of Xinjiang, China (2024-2026).

Appendix A. Supplementary data

Supplementary data to this article can be found online at https://doi.org/10.1016/j.ijbiomac.2024.130453.

References

[1] R.-M. Feng, Y.-N. Zong, S.-M. Cao, R.-H. Xu, Current cancer situation in China: good or bad news from the 2018 Global Cancer Statistics? Cancer Commun. 39 (1) (2019) 22, https://doi.org/10.1186/s40880-019-0368-6.
[2] J. Zhang, Y. Lin, Z. Lin, Q. Wei, J. Qian, R. Ruan, X. Jiang, L. Hou, J. Song, J. Ding, H. Yang, Stimuli-responsive nanoparticles for controlled drug delivery in synergistic cancer immunotherapy, Adv. Sci. 9 (5) (2022) 2103444, https://doi.org/10.1002/advs.202103444.
[3] J. Li, D.J. Mooney, Designing hydrogels for controlled drug delivery, Nat. Rev. Mater. 1 (12) (2016) 16071, https://doi.org/10.1038/natrevmats.2016.71.
[4] H. Almeida, M.H. Amaral, P. Lobão, J.M.S. Lobo, In situ gelling systems: a strategy to improve the bioavailability of ophthalmic pharmaceutical formulations, Drug Discov. Today 19 (4) (2014) 400–412, https://doi.org/10.1016/j.drudis.2013.10.001.
[5] C. Lu, M. Liu, H. Fu, W. Zhang, G. Peng, Y. Zhang, H. Cao, L. Luo, Novel thermosensitive in situ gel based on poloxamer for uterus delivery, Eur. J. Pharm. Sci. 77 (2015) 24–28, https://doi.org/10.1016/j.ejps.2015.05.014.
[6] N.U. Khaliq, K.S. Oh, F.C. Sandra, Y. Joo, J. Lee, Y. Byun, I.-S. Kim, I.C. Kwon, J. H. Seo, S.Y. Kim, S.H. Yuk, Assembly of polymer micelles through the sol-gel

transition for effective cancer therapy, J. Control. Release 255 (2017) 258–269, https://doi.org/10.1016/j.jconrel.2017.04.039.
[7] J.K. Cullen, J.L. Simmons, P.G. Parsons, G.M. Boyle, Topical treatments for skin cancer, Adv. Drug Deliver. Rev. 153 (2020) 54–64, https://doi.org/10.1016/j.addr.2019.11.002.
[8] F. Cui, L. Xi, D. Wang, L. Ren, X. Tan, X. Li, J. Li, T. Li, Advanced in carbon dot-based hydrogels for antibacterial, detection and adsorption, Coordin. Chem. Rev. 497 (2023) 215457, https://doi.org/10.1016/j.ccr.2023.215457.
[9] F. Cui, Y. Ning, D. Wang, J. Li, X. Li, T. Li, Carbon dot-based therapeutics for combating drug-resistant bacteria and biofilm infections in food preservation, Crit. Rev. Food Sci. 64 (2) (2024) 203–219, https://doi.org/10.1080/10408398.2022.2105801.
[10] X. Wu, H. Sun, Z. Qin, P. Che, X. Yi, Q. Yu, H. Zhang, X. Sun, F. Yao, J. Li, Fully physically crosslinked pectin-based hydrogel with high stretchability and toughness for biomedical application, Int. J. Biol. Macromol. 149 (2020) 707–716, https://doi.org/10.1016/j.ijbiomac.2020.01.297.
[11] Y. Liu, J. Liu, S. Chen, T. Lei, Y. Kim, S. Niu, H. Wang, X. Wang, A.M. Foudeh, J. B. Tok, Z. Bao, Soft and elastic hydrogel-based microelectronics for localized low-voltage neuromodulation, Nat. Biomed. Eng. 3 (1) (2019) 58–68, https://doi.org/10.1038/s41551-018-0335-6.
[12] S. Lu, X. Bai, H. Liu, P. Ning, Z. Wang, C. Gao, B. Ni, M. Liu, An injectable and self-healing hydrogel with covalent cross-linking in vivo for cranial bone repair, J. Mater. Chem. B 5 (20) (2017) 3739–3748, https://doi.org/10.1039/C7TB00776K.
[13] Z.Y. Zhao, Z. Wang, G. Li, Z.W. Cai, J.Z. Wu, L. Wang, L.F. Deng, M. Cai, W.G. Cui, Injectable microfluidic hydrogel microspheres for cell and drug delivery, Adv. Funct. Mater. 31 (31) (2021) 2103339, https://doi.org/10.1002/adfm.202103339.
[14] Y. Gu, Y. Yang, J. Yuan, Y. Ni, J. Zhou, M. Si, K. Xia, W. Yuan, C. Xu, S. Xu, Y. Xu, G. Du, D. Zhang, W. Sun, S.Y. Zheng, J. Yang, Polysaccharide-based injectable hydrogels with fast gelation and self-strengthening mechanical kinetics for oral tissue regeneration, Biomacromolecules 24 (7) (2023) 3345–3356, https://doi.org/10.1021/acs.biomac.3c00379.
[15] Y. Liu, L. Dong, Y. Li, Q. Chen, L. Wang, M.A. Farag, L. Liu, S. Zhan, Z. Wu, L. Liu, Soy protein isolate-citrus pectin composite hydrogels induced by TGase and ultrasonic treatment: potential targeted delivery system for probiotics, Food Hydrocolloid. 143 (2023) 108901, https://doi.org/10.1016/j.foodhyd.2023.108901.
[16] Z. Hu, J. Cheng, S. Xu, X. Cheng, J. Zhao, Z.W. Kenny Low, P.L. Chee, Z. Lu, L. Zheng, D. Kai, PVA/pectin composite hydrogels inducing osteogenesis for bone regeneration, Mater. Today Bio 16 (2022) 100431, https://doi.org/10.1016/j.mtbio.2022.100431.
[17] A.S. Prasad, J. Wilson, L.V. Thomas, Designer injectable matrices of photocrosslinkable carboxymethyl cellulose methacrylate based hydrogels as cell carriers for gel type autologous chondrocyte implantation (GACI), Int. J. Biol. Macromol. 224 (2023) 465–482, https://doi.org/10.1016/j.ijbiomac.2022.10.137.
[18] Z. Pourmanouchehri, S. Ebrahimi, M. Limoee, F. Jalilian, S. Janfaza, A. Vosoughi, L. Behbood, Controlled release of 5-fluorouracil to melanoma cells using a hydrogel/micelle composites based on deoxycholic acid and carboxymethyl chitosan, Int. J. Biol. Macromol. 206 (2022) 159–166, https://doi.org/10.1016/j.ijbiomac.2022.02.096.
[19] F. Cui, S. Zheng, D. Wang, X. Tan, Q. Li, J. Li, T. Li, Recent advances in shelf life prediction models for monitoring food quality, Compr. Rev. Food Sci. F. 22 (2) (2023) 1257–1284.
[20] C. Mo, L. Xiang, Y. Chen, Advances in injectable and self-healing polysaccharide hydrogel based on the Schiff Base reaction, Macromol. Rapid Commun. 42 (10) (2021) e2100025, https://doi.org/10.1002/marc.202100025.
[21] Y. Liang, Z. Li, Y. Huang, R. Yu, B. Guo, Dual-dynamic-bond cross-linked antibacterial adhesive hydrogel sealants with on-demand removability for post-wound-closure and infected wound healing, ACS Nano 15 (4) (2021) 7078–7093, https://doi.org/10.1021/acsnano.1c00204.
[22] C.-H. Lu, C.-H. Yu, Y.-C. Yeh, Engineering nanocomposite hydrogels using dynamic bonds, Acta Biomater. 130 (2021) 66–79, https://doi.org/10.1016/j.actbio.2021.05.055.
[23] M. Rizwan, A.E.G. Baker, M.S. Shoichet, Designing hydrogels for 3D cell culture using dynamic covalent crosslinking, Adv. Healthc. Mater. 10 (12) (2021) 2100234.
[24] Y. Zeng, C. Zhang, D. Du, Y. Li, L. Sun, Y. Han, X. He, J. Dai, L. Shi, Metal-organic framework-based hydrogel with structurally dynamic properties as a stimuli-responsive localized drug delivery system for cancer therapy, Acta Biomater. 145 (2022) 43–51, https://doi.org/10.1016/j.actbio.2022.04.003.
[25] R. Antony, T. Arun, S.T.D. Manickam, A review on applications of chitosan-based Schiff bases, Int. J. Biol. Macromol. 129 (2019) 615–633, https://doi.org/10.1016/j.ijbiomac.2019.02.047.
[26] J.-Q. Zhang, H.-C. Li, J. Wang, S.-S. Liu, J. Li, D.-Q. Li, Dopamine-functionalized pectin-based Pickering emulsion as an oral drug delivery system, Colloid. Surface. A 673 (2023) 131807, https://doi.org/10.1016/j.colsurfa.2023.131807.
[27] S.-Y. Wang, M. Tohti, J.-Q. Zhang, J. Li, D.-Q. Li, Acylhydrazone-derived whole pectin-based hydrogel as an injectable drug delivery system, Int. J. Biol. Macromol. 251 (2023) 126276.
[28] D.-Q. Li, S.-Y. Wang, Y.-J. Meng, J.-F. Li, J. Li, An injectable, self-healing hydrogel system from oxidized pectin/chitosan/gamma-Fe_2O_3, Int. J. Biol. Macromol. 164 (2020) 4566–4574, https://doi.org/10.1016/j.ijbiomac.2023.126276.
[29] J. Chen, Z. Zhai, K.J. Edgar, Recent advances in polysaccharide-based in situ forming hydrogels, Curr. Opin. Chem. Biol. 70 (2022) 102200, https://doi.org/10.1016/j.cbpa.2022.102200.
[30] D. Li, S. Wang, Y. Meng, Z. Guo, M. Cheng, J. Li, Fabrication of self-healing pectin/chitosan hybrid hydrogel via Diels-Alder reactions for drug delivery with high swelling property, pH-responsiveness, and cytocompatibility, Carbohyd. Polym. 268 (2021) 118244, https://doi.org/10.1016/j.carbpol.2021.118244.
[31] P. Perrone, C.M. Hewage, A.R. Thomson, K. Bailey, I.H. Sadler, S.C. Fry, Patterns of methyl and O-acetyl esterification in spinach pectins: new complexity, Phytochemistry 60 (1) (2002) 67–77, https://doi.org/10.1016/S0031-9422(02)00039-0.
[32] L. Zhang, X. Ye, T. Ding, X. Sun, Y. Xu, D. Liu, Ultrasound effects on the degradation kinetics, structure and rheological properties of apple pectin, Ultrason. Sonochem. 20 (1) (2013) 222–231, https://doi.org/10.1016/j.ultsonch.2012.07.021.
[33] H. An, Y. Yang, Z. Zhou, Y. Bo, Y. Wang, Y. He, D. Wang, J. Qin, Pectin-based injectable and biodegradable self-healing hydrogels for enhanced synergistic anticancer therapy, Acta Biomater. 131 (2021) 149–161, https://doi.org/10.1016/j.actbio.2021.06.029.
[34] M. Kratchanova, A. Slavov, C. Kratchanov, Interaction of pectin with amino acids and other amino compounds in aqueous solution, Food Hydrocolloid. 18 (4) (2004) 677–683, https://doi.org/10.1016/j.foodhyd.2003.11.004.
[35] P. Li, Y. Sui, X. Dai, Q. Fang, H. Sima, C. Zhang, Dynamic tannic acid hydrogel with self-healing and pH sensitivity for controlled release, Macromol. Biosci. 21 (6) (2021) e2100055, https://doi.org/10.1002/mabi.202100055.
[36] Y. Shitrit, M. Davidovich-Pinhas, H. Bianco-Peled, Shear thinning pectin hydrogels physically cross-linked with chitosan nanogels, Carbohyd. Polym. 225 (2019) 115249, https://doi.org/10.1016/j.carbpol.2019.115249.
[37] K. Bu, D. Huang, D. Li, C. Zhu, Encapsulation and sustained release of curcumin by hawthorn pectin and Tenebrio Molitor protein composite hydrogel, Int. J. Biol. Macromol. 222 (2022) 251–261, https://doi.org/10.1016/j.ijbiomac.2022.09.145.
[38] N.-G. Kim, P. Chandika, S.-C. Kim, D.-H. Won, W.S. Park, I.-W. Choi, S.G. Lee, Y.-M. Kim, W.-K. Jung, Fabrication and characterization of ferric ion cross-linked hyaluronic acid/pectin-based injectable hydrogel with antibacterial ability, Polymer 271 (2023) 125808, https://doi.org/10.1016/j.polymer.2023.125808.
[39] M. Wu, J. Chen, W. Huang, B. Yan, Q. Peng, J. Liu, L. Chen, H. Zeng, Injectable and self-healing nanocomposite hydrogels with ultrasensitive pH-responsiveness and tunable mechanical properties: implications for controlled drug delivery, Biomacromolecules 21 (6) (2020) 2409–2420, https://doi.org/10.1021/acs.biomac.0c00347.
[40] F. Seidi, R. Jenjob, D. Crespy, Designing smart polymer conjugates for controlled release of payloads, Chem.l Rev. 118 (7) (2018) 3965–4036, https://doi.org/10.1021/acs.chemrev.8b00006.
[41] E.H. Cordes, W.P. Jencks, On the mechanism of Schiff Base formation and hydrolysis, J. Am. Chem. Soc. 84 (5) (1962) 832–837, https://doi.org/10.1021/ja00864a031.
[42] S. Khan, N. Akhtar, M.U. Minhas, S.F. Badshah, pH/Thermo-dual responsive tunable in situ cross-linkable depot injectable hydrogels based on poly(N-Isopropylacrylamide)/carboxymethyl chitosan with potential of controlled localized and systemic drug delivery, AAPS PharmSciTech 20 (3) (2019) 119, https://doi.org/10.1208/s12249-019-1328-9.
[43] A. Anitha, K.P. Chennazhi, S.V. Nair, R. Jayakumar, 5-Flourouracil Loaded N,O-Carboxymethyl Chitosan Nanoparticles as an Anticancer Nanomedicine for Breast Cancer, J. Biomed. Nanotechnol. 8 (1) (2012) 29–42, https://doi.org/10.1166/jbn.2012.1365.
[44] A.S. Vaziri, I. Alemzadeh, M. Vossoughi, A.C. Khorasani, Co-microencapsulation of lactobacillus plantarum and DHA fatty acid in alginate-pectin-gelatin biocomposites, Carbohyd. Polym. 199 (2018) 266–275, https://doi.org/10.1016/j.carbpol.2018.07.002.